

## Cathode region of a transitory discharge in CO<sub>2</sub>. II. Spatio-temporal evolution

P. Bayle, J. Vacquie, and M. Bayle

*Laboratoire de Génie Electrique, Université Paul Sabatier, 118 Route de Narbonne, 31062 Toulouse Cédex, France*

(Received 12 December 1985)

The inception of the cathode region is described by a second-order hydrodynamic model proposed in the preceding paper. The spatio-temporal variations of ionic and electronic densities, electron temperature, electron pressure, and electric field are provided. The double nonequilibrium between the electrons and the electric field due to strong electric field gradients and to secondary emission at the cathode is carefully studied. The way these electrons emitted by the cathode join the discharge is studied as a function of their emission temperature. The evolution of the electron temperature shows a maximum shifted from the field maximum. This leads to a difference between the non-equilibrium apparent ionization coefficient (deduced from the dynamic temperature) and the corresponding equilibrium coefficient. The maximum drop of the electric field and almost the main part of the processes that sustain the discharge occur in the transition zone situated between the cathode fall and the negative glow. In this zone, the electron energy density (electron pressure) is maximum involving a maximum in the reaction rates (the ionization, excitation rates, and the electron current density are maximum). When the electron current density increases, the electric field at the cathode increases as the cathode-fall length decreases.

### I. INTRODUCTION

In the preceding paper, hereafter designated as I (Bayle, Vacquie, and Bayle<sup>1</sup>), we have proposed and analyzed a formalism for the study of the cathode region in transitory discharges. This formalism is based on the equations of hydrodynamics for a slightly ionized gas (continuity equations for electrons and ions, momentum and energy equations for electrons). A formulation of the source terms of the continuity equations and of the operators of collisional transfer for momentum and energy was chosen. In paper I, we mainly focused on the analysis of the formalism and on the role of the different terms of the equations, i.e., on the role of the physical processes they represent. The detailed analysis of these equations showed the role played by the electric field as a source of energy and the collective phenomena (total diffusion and electron pressure work) as regulating mechanisms of the discharge, in the inception of the cathode-fall region and of the negative glow.

In this paper (II), we will deal particularly with the spatio-temporal evolution of the cathode region (cathode fall and negative glow), together with the study of the main processes (ionization, excitation, and transport) arising from the energetic nonequilibrium between the electrons and the electric field. The main different zones of the cathode region are characterized by their energetic properties and by the electric field repartition.

Special care will be given to the two transition zones of the cathode region. The first transition zone is the part of the discharge in contact with the cathode, which shows a double nonequilibrium between the electrons and the electric field; this nonequilibrium depends first on the strong gradients of the electric field and secondly on the difference between the energy of the electrons emitted by the cathode and that of the electrons of the discharge.

The second transition zone is the part of the discharge lying between the cathode fall (CF) and the negative glow (NG). In this zone, the main sustaining processes of the discharge take place.

### II. SPATIO-TEMPORAL EVOLUTION OF THE CATHODE REGION

Apart from Figs. 13 and 14, all the figures in this paper are drawn for an emission temperature of 5 eV for secondary electrons.

#### A. Electric field and densities

The initial conditions are defined in I in Fig. 1, electric field being chosen linearly decreasing in the studied area. This initial repartition is greatly modified by the double action of the space-charge effects and nonequilibrium between electrons and the electric field. Figure 1 shows the spatio-temporal evolution of the electron density, which first increases exponentially from the cathode, then varies very little in the following zone. A difference may be noticed between curve 1 and the other curves; it is linked to the initial conditions in which the cathode fall lies all over the studied area without negative glow. It implies a different action of the feedback of collective phenomena (role of the spatial gradients in the momentum and energy equations). At the beginning, the transport phenomena are stronger than the ionization, and near the cathode where the electron velocity is high, this induces an electron density decrease (from curve 1 to curve 2). Then, the ionization becomes higher than the transport phenomena and the electron density increases regularly as shown on curve 2. From this moment, the evolution of the electron density appears as the result of the ionization mechanisms (a function of the electron temperature) and of the trans-

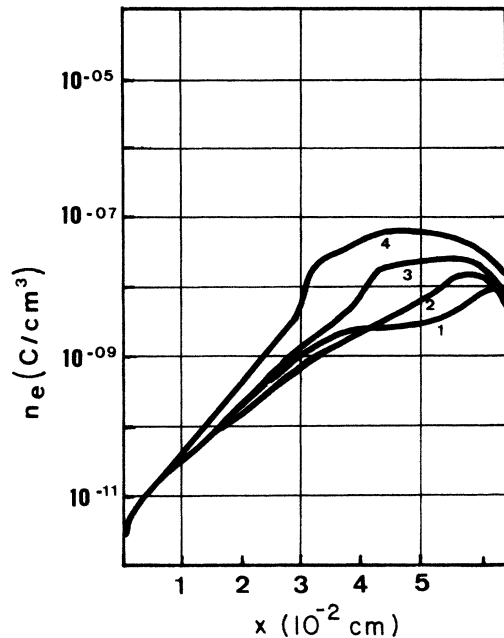


FIG. 1. Spatio-temporal evolution of the electron density. (1)  $t=0.5$  ns, (2)  $t=1.6$  ns, (3)  $t=5.4$  ns, (4)  $t=13$  ns. (The abscissa is the distance from the cathode.)

port processes sweeping away the electrons to the anodic boundary of the region. Then, the NG appears as the result of a gradient effect and the electron velocity decreases sharply in the transition zone from the CF and the NG. This decrease of the electron velocity induces a local increase of the electron density although the attachment is high. Curves 2–4 in Fig. 1 show how, at the beginning of the NG the electron density increases, thus indicating a progressive gathering of the electrons in the NG due to a decrease of the electron velocity. So, the NG appears gradually and the total diffusion effects cause more and more decrease of the electron velocity. They move more and more slowly at the beginning of the NG and this slowing down causes a widening of the NG.

The evolution of the density of the negative ions is similar to that of the electrons (Fig. 2). It is governed by attachment processes, which are mostly significant at the beginning of the NG. Figure 3 shows the evolution of the CO<sub>2</sub><sup>+</sup> positive ions created by ionization. As their drift velocity is weak, they move much more slowly than electrons. In the transition zone, the transport phenomenon of CO<sub>2</sub><sup>+</sup> ions shows a sharp variation linked to a steep decrease of the electric field. On both sides of the transition zone, the velocity of CO<sub>2</sub><sup>+</sup> ions is nearly constant while in the transition zone, it increases sharply so that the CO<sub>2</sub><sup>+</sup> positive ions enter the CF with a high kinetic energy. As the transport phenomena are very different for electrons and ions, the net space-charge evolution shows an increasing excess of CO<sub>2</sub><sup>+</sup> positive ions in the CF, whereas the electrons drifting under the electric field action gather in the NG. Thus the net space-charge density, becoming positive in the CF and negative in the NG induces a strong decrease of the electric field in the transition zone between the CF and the NG. The net space-charge den-

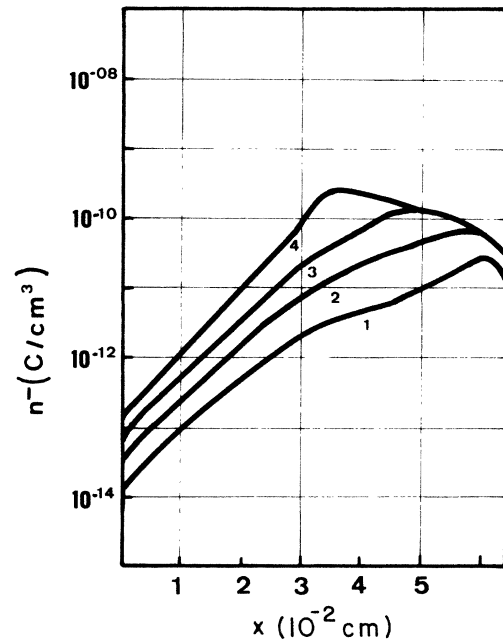


FIG. 2. Spatio-temporal evolution of the negative-ion density. (1)  $t=0.5$  ns, (2)  $t=1.6$  ns, (3)  $t=5.4$  ns, (4)  $t=13$  ns.

ty is positive again on the anode side of the cathode region.

Figure 4 shows the spatio-temporal evolution of the electric field. The inception of the NG and the narrowing of the cathode fall in time are obvious. In the NG, the electric field decreases steeply as the electric field reaches the lowest value available in the computation (10 V/cm). This value corresponds to a zero-field value for the physical phenomena in the discharge, as there is no drift and no

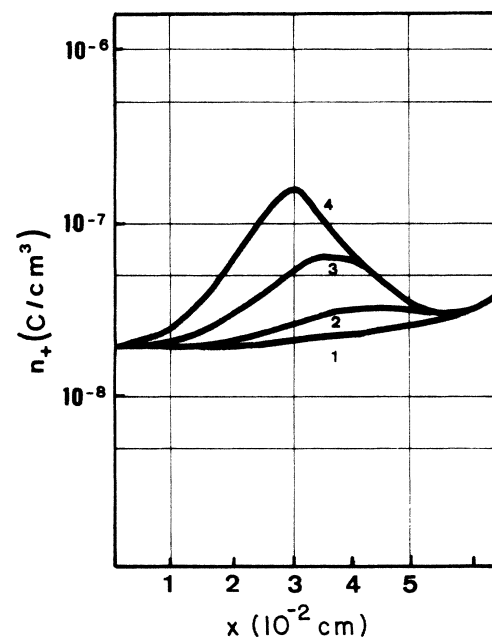


FIG. 3. Spatio-temporal evolution of the positive-ion density. (1)  $t=0.5$  ns, (2)  $t=1.6$  ns, (3)  $t=5.4$  ns, (4)  $t=13$  ns.

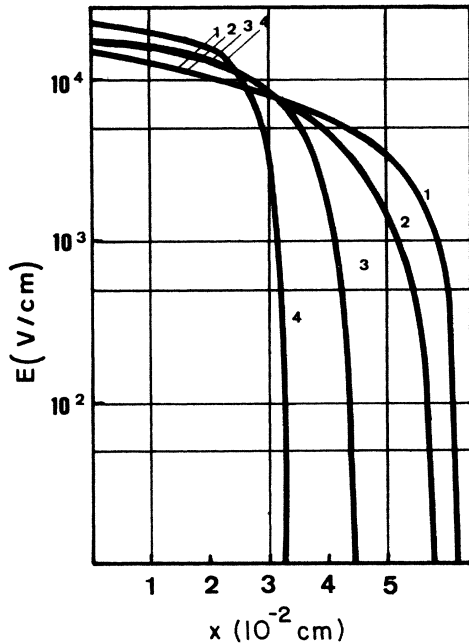


FIG. 4. Spatio-temporal evolution of the electric field. (1)  $t = 0.5$  ns, (2)  $t = 1.6$  ns, (3)  $t = 5.4$  ns, (4)  $t = 13$  ns.

electron multiplication. The practical formulation of the hydrodynamic equations together with the numerical technique for their resolution do not allow one to deal with zero-field values and even less with field inversions.

Figure 5 shows the spatio-temporal evolution of the electron temperature. The electron temperature maximum is situated just before the cathode and not on the cathode itself as it is for the field maximum. This is a

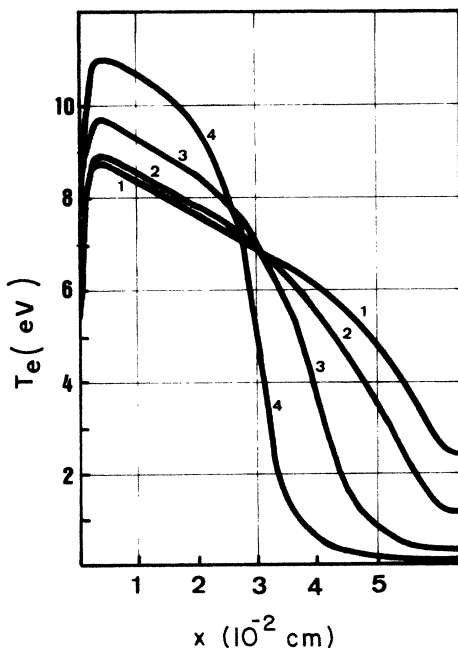


FIG. 5. Spatio-temporal evolution of the electron temperature. (1)  $t = 0.5$  ns, (2)  $t = 1.6$  ns, (3)  $t = 5.4$  ns, (4)  $t = 13$  ns.

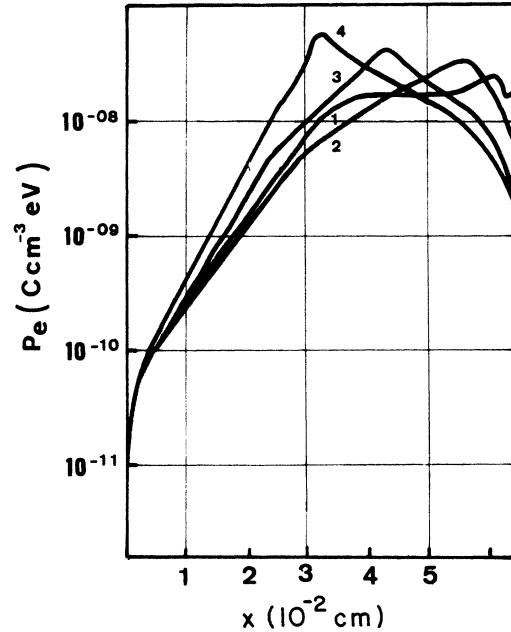


FIG. 6. Spatio-temporal evolution of the electron pressure. (1)  $t = 0.5$  ns, (2)  $t = 1.6$  ns, (3)  $t = 5.4$  ns, (4)  $t = 13$  ns.

first sign of nonequilibrium between the electrons and the electric field. It is clear that the evolution of the dynamic temperature deduced from the energy equation does not follow the evolution of the electric field as it is for the static temperature.

Figure 6 shows the spatio-temporal evolution of the electron pressure (electron energy density) and gives a global view of the discharge evolution. The energy of the electron gas increases all along the CF under the electric field action and the maximum in the energy density is situated in the transition zone. In the NG, where the electric field is weak, the electron gas does not gain energy but loses it by collisions. So gain and loss of energy characterize, respectively, the CF and the NG.

## B. Nonequilibrium between the electrons and the electric field

The strong gradients appearing in the cathode region, and particularly in the transition zone between the cathode fall and the negative glow, are one of the particularities of the cathode region. The diffusion processes imply that the energetic behavior of electrons is not only a function of the electric field alone but also a function of the whole structure of the discharge. This phenomenon induces the nonequilibrium between the electrons and the electric field.

### 1. Effect on the electron temperature

Figure 7 shows the spatial distribution of the mean dynamic local temperature in the cathode region (a) compared to the distribution of the static local temperature (b) deduced from the equilibrium field-temperature relation [Eq. (25) of I]. This temperature represents the mean

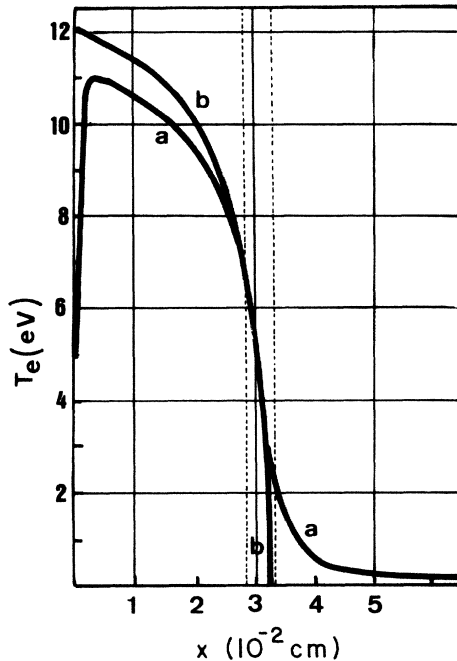


FIG. 7. Spatial distribution of (a) the dynamic electron temperature and (b) the static electron temperature.

temperature of an electron submitted to the same value of the electric field in a stationary and uniform discharge.

On Fig. 7, a strong nonequilibrium zone appears near the cathode due to the two reasons previously described: first, the emission temperature of the electrons ejected from the cathode, and secondly, the discontinuity introduced by the cathode itself (absorbing wall for ions). In this zone, the dynamic temperature is lower than the static one. The maximum in the dynamic temperature is shifted from the electric field maximum that takes place at the cathode. This means that the maximum of the ionization frequency does not take place on the cathode but just in front of it, at a distance where the secondary electrons ejected have reached the mean temperature of the electron swarm. The dynamic electron temperature decreases because the electric field decreases and thus provides less energy to electrons. In the transition zone between CF and NG, the energy gain and loss nearly balance and the electron temperature is nearly equal to the static temperature.

In the negative glow, a weak electric field region, the collision losses are the greatest energy loss, whereas the electron pressure work maintains the electron energy so that in spite of a nearly null electric field, electrons have a non-null energy and the nonequilibrium gives rise to a dynamic temperature higher than the static temperature.

## 2. Effect on the electron velocity

The effect of nonequilibrium on the electron velocity is shown by the comparison between the total velocity and the drift velocity. The cathode fall appears as a weak nonequilibrium region, the drift velocity being quite equal to the total velocity. This means that the velocity gain

under the field action is much stronger than the loss by diffusion and collisions. The electron velocity in the CF nearly depends on the electric field alone following all of its variations. On the contrary, in the NG, where the electric field is nearly null, the drift velocity is null but the total diffusion velocity is not null. So, the NG appears as a strong nonequilibrium region where the total diffusion effects balance the electric field lack and the collision loss. In this region, the electron velocity is a diffusion velocity which is corroborated by a term-to-term analysis of the momentum equation showing that the diffusion term is the most significant.

## C. Ionization and excitation mechanisms

The electric field and the dynamic electron temperature configurations lead to a repartition of the collision frequency, of the ionization, attachment and excitation frequencies in the cathode region (Fig. 8). The momentum-transfer frequency (curve 1) shows a weak variation, whereas the others sharply vary by several orders of magnitude. The ionization frequency (curve 3) increases from the cathode and reaches rapidly its maximum value which remains nearly constant in the CF. It decreases strongly in the transition zone and reaches a nearly null value in the NG, where the electric field and the electron temperature are too weak for the electrons to ionize. A similar variation is observed for the excitation frequency (curve 2). The attachment frequency (curve 4) is maximum near the cathode, increasing the relative part of the positive-ion component in the total current near the cathode. Then, it remains nearly constant in the CF and shows a weak maximum when the electron energy decreases in the transition zone.

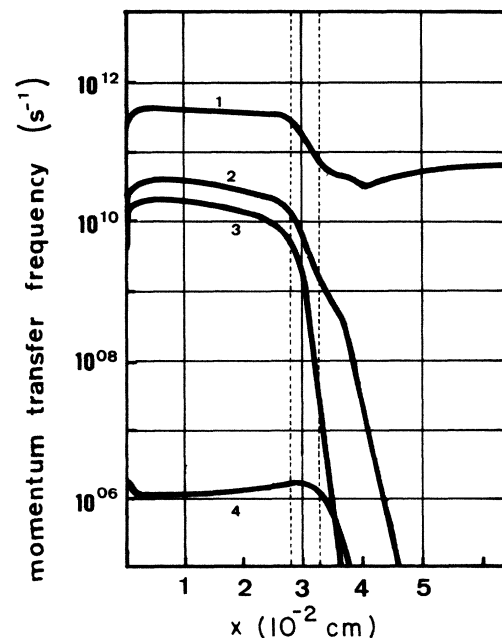


FIG. 8. Momentum transfer frequency by collisions (1), excitation frequency (2), ionization frequency (3), attachment frequency (4),  $t = 13$  ns.

Figure 9 shows the collision rate (product of the collision frequency by the electron density). The collisions have a major role in the NG, they appear as the most significant process in this zone. It is obvious that the major part of the ionization and excitation processes do not take place in the CF, even if it is a place with a strong electric field and a high electron temperature, but takes place in the transition zone, a place with moderate field and temperature. The production of electrons by ionization is weak in the CF, then increases and reaches its maximum value in a weak electric field zone (this is the result of the exponential increase of the electron density in the CF). In this zone, the attachment is the highest and at the beginning of the NG, the attachment is greater than ionization. A similar conclusion about maxima in ionization and excitation on the cathode side of the negative glow, i.e., in a nearly null electric field region is given by Warren<sup>2</sup> in experimental results.

Figure 10 represents the evolution of the electronic current density and of the positive current density. The positive-ion current is the main component of the total current density at the cathode and in the CF, then it decreases very fast in the transition zone following the decrease of the electric field and the positive-ion velocity and is nearly negligible in the NG. In the NG, the main part of the current is electronic. This is linked both to the very strong increase of electron density and to the ratio of the electronic and ionic velocities which increases in this zone. The current is higher at the end of the CF and in the transition zone, where the electric field and the electron temperature are high enough to sustain a significant electron and ion transport. In the NG where the electric field and the electron temperature decrease, the electron transport is weak and the current density decreases.

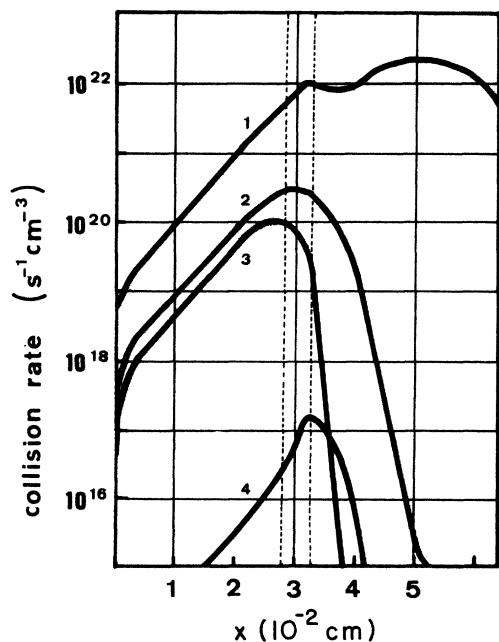


FIG. 9. Collision rate (1), excitation rate (2), ionization rate (3), attachment rate (4),  $t = 13$  ns.

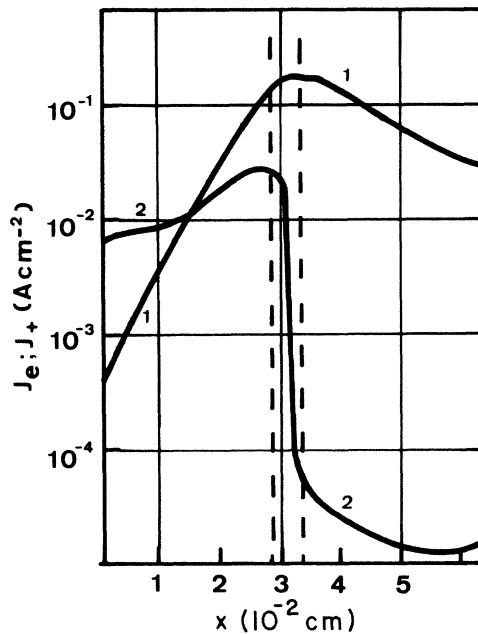


FIG. 10. Electronic current density (1), positive ionic current density (2),  $t = 13$  ns.

The electronic amplification  $M(x,t) = J_e(x,t)/J_e(0,t)$  reaches a maximum in the transition zone (Fig. 11). Figure 12 shows the effect of nonequilibrium on the macroscopic coefficients as the apparent ionization coefficient. The apparent ionization coefficient deduced from the ionization and attachment source terms [Eqs. (20) and (21) of I] by the following relation in which the dynamic temperature is involved:

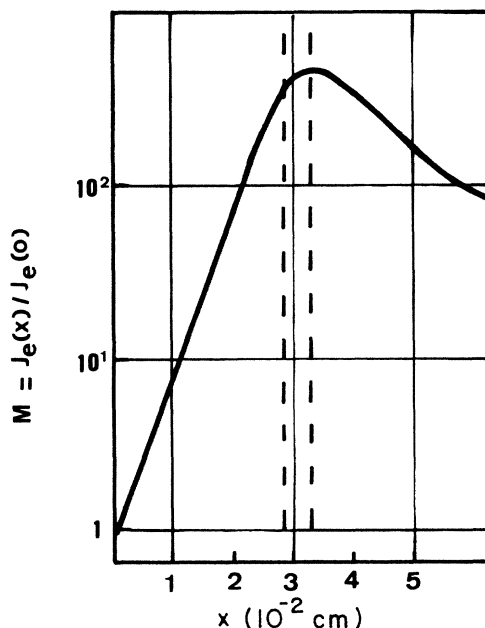


FIG. 11. Electronic amplification  $M = J_e(x)/J_e(0)$ ,  $t = 13$  ns.

$$S_{\text{ion}}(T_e, n_e, N) - S_{\text{att}}(T_e, n_e, N) = \frac{\lambda^{(\text{NE})}}{N}(T_e) N n_e u_e(T_e)$$

is compared to the apparent Townsend coefficient deduced from the current measurements in homogeneous

and stationary discharges. This equilibrium coefficient is deduced from Dutton<sup>3</sup> and Kucukarpaci and Lucas<sup>4</sup> and Gallagher *et al.*<sup>5</sup> It only depends on the electric field and is used on the following form at 293 K:

$$E/N > 364 \text{ Td}, \quad \lambda^{(E)}/N = 6.277 \times 10^{-16} \exp \left[ \frac{-1.623 \times 10^3}{(E/N)} + \frac{2.614 \times 10^5}{(E/N)^2} \right],$$

$$136 \text{ Td} < E/N \leq 364 \text{ Td}, \quad \lambda^{(E)}/N = -1.556 \times 10^{-17} + 1.751 \times 10^{-19}(E/N),$$

$$E/N \leq 136 \text{ Td}, \quad \lambda^{(E)}/N = -4.092 \times 10^{-20}(E/N) + 7.492 \times 10^{-22} (E/N)^2.$$

There is a strong difference between their values, particularly near the cathode. In this zone, the nonequilibrium is the strongest as the electrons ejected by the cathode have an energy unconnected with the local energy of the electron swarm. Whereas the apparent ionization coefficient  $\lambda^{(E)}(E/N)$  in an equilibrium situation follows strictly the field decrease, the nonequilibrium coefficient  $\lambda^{(\text{NE})}(T_e)$ , which is the real one in the discharge, reaches a maximum value near the cathode. In the CF,  $\lambda^{(\text{NE})}(T_e)$  is lower than  $\lambda^{(E)}(E/N)$ , showing that nonequilibrium reduces the ionizing rate of the electrons in this zone compared to the classic equilibrium modeling. In the CF-NG transition zone, it is the contrary and  $\lambda^{(\text{NE})}(T_e)$  becomes higher than  $\lambda^{(E)}(E/N)$ . In fact, in this zone, the electronic multiplication is the highest (Fig. 11).

### III. THE TRANSITION ZONES IN THE CATHODE REGION

#### A. Cathodic processes

This zone is mainly the adjustment zone for secondary electrons to reach the local conditions taking place in the gas ahead of the cathode. Generally, these electrons are supposed to be ejected with an energy ranging from 0 to 20 eV (Von Engel,<sup>6</sup> Ohuchi and Kubota,<sup>7</sup> Marode and Boeuf.)<sup>8</sup> How these electrons adjust their emission conditions to the electric field and the electron pressure conditions taking place near the cathode seems to be interesting. Figures 13 and 14 show the mean electron velocity  $u_e$  and the dynamic electron temperature  $T_e$  near the cathode. In the range of emission temperature chosen, the velocity and the energy of the secondary electrons adjust at the same distance from the cathode, whatever the value of the emission temperature. Of course, these curves are drawn in the same conditions of electric field and charge

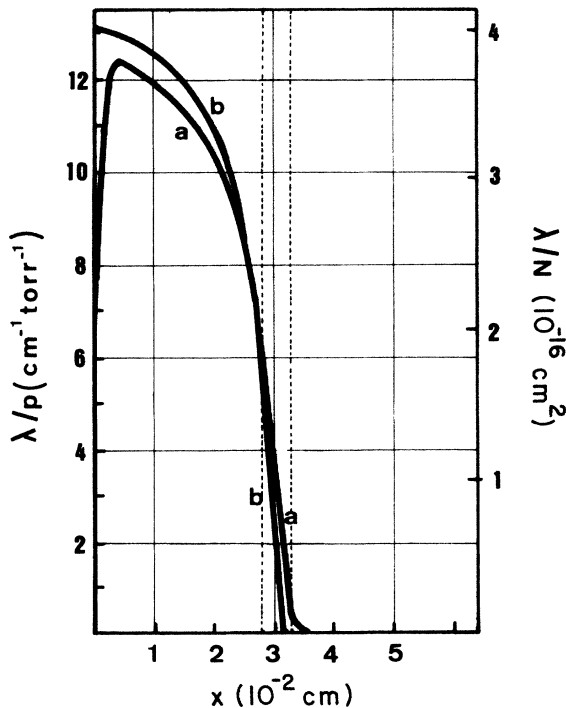


FIG. 12. Comparison between the apparent ionization coefficient (a) in a nonequilibrium situation  $\lambda^{(\text{NE})}/N = f(T_e)$ , and (b) in an equilibrium situation  $\lambda^{(E)}/N = f(E)$ .

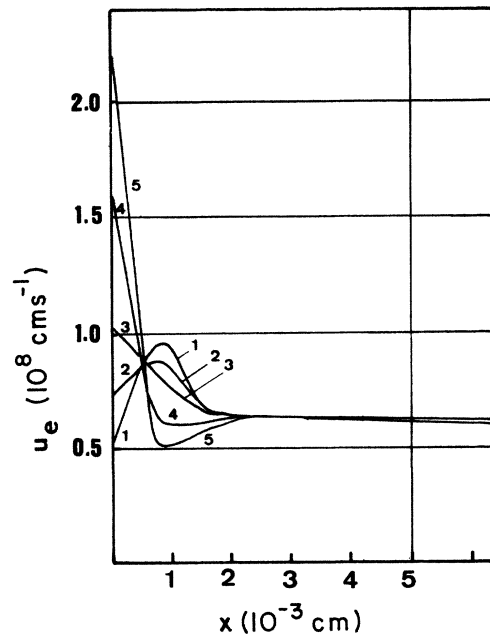


FIG. 13. Mean electron velocity near the cathode  $t=2$  ns. (1)  $T_e=0.5$  eV, (2)  $T_e=1$  eV, (3)  $T_e=2$  eV, (4)  $T_e=5$  eV, (5)  $T_e=10$  eV.

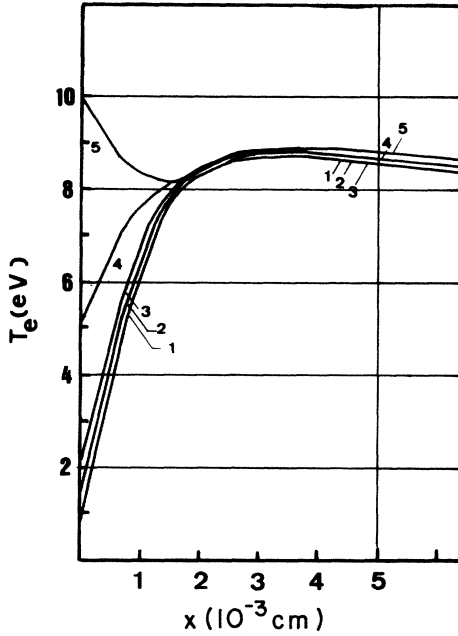


FIG. 14. Mean electron temperature near the cathode  $t = 2$  ns. (1)  $T_e = 0.5$  eV, (2)  $T_e = 1$  eV, (3)  $T_e = 2$  eV, (4)  $T_e = 5$  eV, (5)  $T_e = 10$  eV.

carrier density. This means that the secondary electrons “forget” very soon their emission conditions to fit the local conditions of the electron swarm. Only 5% of the total length of the cathode region are necessary to stabilize those values. We must notice that the adjustment distance is the same for the different emission conditions and moreover that the adjustment value is the same for the velocity. As for energy (Fig. 14), there is a slight difference in the adjustment value if the electrons emitted by the cathode have energies equal to or greater than 5 eV.

The way this stabilization occurs can be analyzed accurately by a comparison of the different physical processes (role of the electric field, diffusion and ionization processes, . . .), i.e., by a study of the different terms of the momentum and energy equations as was done in I. The collective phenomena (total diffusion) [curve 2 in Fig. 15(a)] are the more significant processes. The total diffusion term in the momentum equation varies by an order of magnitude on the adjustment distance and reduces the velocity when it is too high, whereas on the same distance, the velocity gain due to the electric field (curve 1) remains nearly constant. In the energy equation, a similar variation occurs. The term corresponding to the energy gain due to the electric field [curve 1 of 15(b)] shows a slight variation on the adjustment distance, whereas the term corresponding to the electron pressure work (curve 2) varies more as the difference between the secondary emission temperature and the mean local temperature is great. This shows the significant role played by the collective phenomena as stabilizing processes in the discharge.

This zone is the strongest nonequilibrium area with a dynamic temperature half of the static temperature. The adjustment for temperature occurs for higher values when the emission temperature increases (Fig. 14). As the

source terms sharply vary with the temperature, this difference can induce great variations of the electron multiplication and of the net space charge at the boundary between the CF and the NG and in the NG itself. On the contrary, few variations of the net space charge and the electric field at the cathode are induced. The temporal

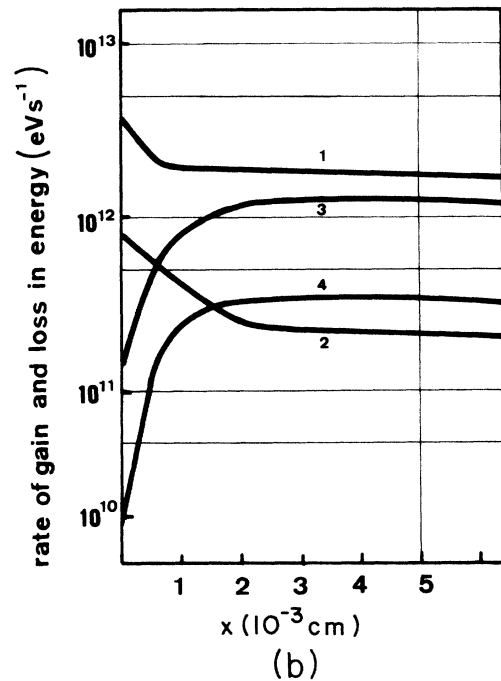
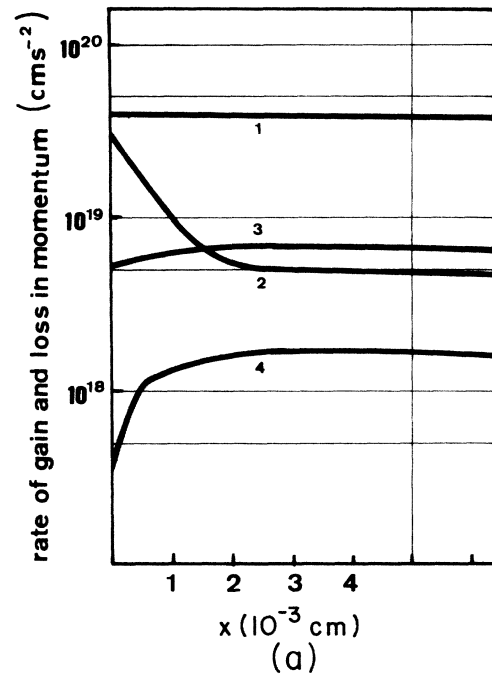


FIG. 15. (a) Comparison between the different terms of the momentum equation near the cathode  $t = 13$  ns; (1)  $(e/m_e)E$ , (2)  $(e/m_e)(1/n_e)[\partial(n_e T_e)/\partial x]$ , (3)  $v[\psi(T_e)]u_e$ , (4)  $(S_{ion} - S_{att}/n_e)u_e$ . (b) Comparison between the different terms of the energy equation near the cathode  $t = 13$  ns; (1)  $u_e E$ , (2)  $(1/n_e)[\partial(n_e T_e u_e)/\partial x]$ , (3)  $(1/n_e)(\nabla^e + \nabla^i)\frac{1}{2}m_e w_e^2$ , (4)  $\frac{3}{2}T_e(S_{ion} - S_{att})/n_e$ .

evolution of the electric field the cathode is shown on Fig. 16. It increases regularly with time, whatever the emission temperature.

### B. The transition zone between the cathode fall and the negative glow

The transition zone between the CF and the NG plays a major role in the discharge. The prevailing role of the electric field comes to an end long before it reaches its lower value. In fact, the discharge properties are modified as soon as the role of the collective phenomena is reversed, i.e., when the spatial gradients in the momentum and the energy equations change their signs. Therefore, the transition zone can be stated as a zone of inversion of collective phenomena. Its spatial boundaries are the zone where the terms corresponding to these phenomena are null. On the cathode side, the boundary is defined as  $\partial(n_e T_e u_e)/\partial x = 0$ , i.e., in the area where the electron energy seems to depend only on the gain under the field action and on the loss by collisions and does not depend on the discharge structure. On the anode side, the boundary with the negative glow is defined as the place where  $\partial(n_e T_e)/\partial x = 0$ , that is, the total diffusion velocity is equal to zero.

This transition zone position evolves with time and reduces the extension zone of the CF region (Fig. 17). At the same time, the current density increases. These results corroborate fully Warren's results,<sup>2</sup> who found experimentally a decrease of the cathode-fall region and Ward's<sup>9</sup> results, who studied a stationary discharge by a first-order model and found a decrease of the length of the CF region with an increase of the current density.

In the transition zone, different processes reach their

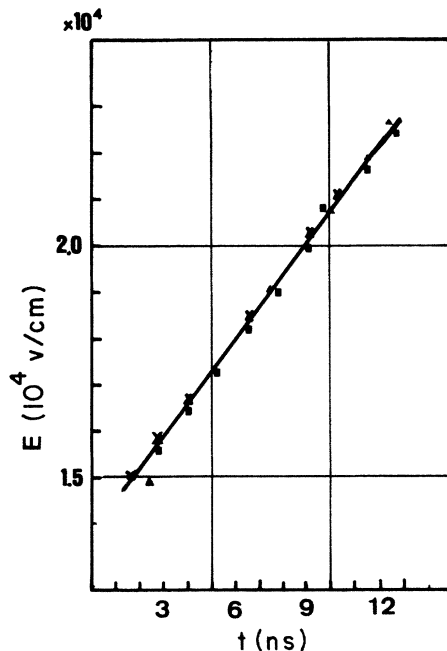


FIG. 16. Temporal evolution of the electric field at the cathode.

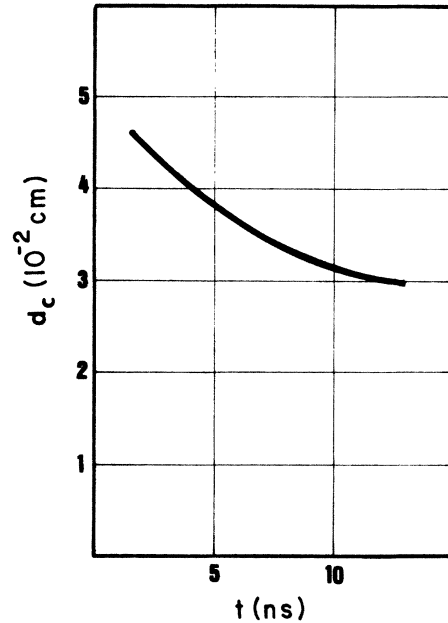


FIG. 17. Temporal evolution of the cathode-fall length.

higher values. It is the place of highest electron multiplication (Fig. 11), of highest ionization, energy density, and excitation rates (Fig. 9). In the transition zone, the electrons are in equilibrium with the electric field.

The two zones of the cathode region, CF and NG, are thus defined in term of energetic evaluation. The definition of the transitory zone between CF and NG appears as the inversion place of the collective phenomena and generalizes the classic definition of the CF and NG in terms of field variation. In the transition zone, the field gradients are the strongest and the discharge enhancement is maximum.

## V. CONCLUSION

The inception and the development of the cathode region are mainly governed by the energetic mechanisms resulting from the energy gain due to the electric field and collective phenomena actions, that is, the total diffusion and the work of electron pressure. The inversion of the action of the collective phenomena induces the change from one zone of the cathode region to the other. This allows one to define these two zones by their energetic properties.

### A. The cathode-fall region

The cathode-fall region is a high electric field region. The electric field is maximum on the cathode and decreases all along the CF. Elastic collisions and electron pressure work decrease the electron temperature sustained by the electric field action. The nonequilibrium between the electrons and the electric field is the strongest in this zone and gives rise to a maximum in the electron temperature shifted down from the field maximum. The elec-



tron temperature is high and the electron multiplication increases progressively. The current is mainly a positive ionic current.

The secondary emission at the cathode due to ionic impact is the main secondary process. These secondary electrons are ejected with a temperature very different from the local electron temperature in the gas. According to their emission temperature, they gain energy under the electric field action or lose it under different processes such as elastic or inelastic collisions, feedback of electron pressure work.

The cathode-fall region is a zone where the active phenomena of the discharge occur: ionization, attachment, and diffusion (towards the cathode). The cathode-fall length decreases when the current density increases but the maximum of the electron energy density always takes place in the transition zone. In the transition zone the re-

action rates are the strongest and the action of collective phenomena is reversed.

#### B. The negative glow region

By contrast with the cathode-fall region the negative-glow region appears as a weak, nearly null electric field region and the electron energy is only sustained by the electron pressure work linked to the spatial configuration of the energy density. The velocity is weak and sustained by the diffusion towards the anode. This zone plays a regulating and stabilizing role on the electron velocity. In this region, there is little ionization, and the negative-ion density is the highest, inducing a weak electric field increase just in front of the positive column. In this area, the elastic collisions rate is most significant and remains nearly constant. It tends to reduce the electron velocity.

---

<sup>1</sup>P. Bayle, J. Vacquie, and M. Bayle, *Phys. Rev. A* **34**, 360 (1986).

<sup>2</sup>R. Warren, *Phys. Rev.* **98**, 1650 (1955).

<sup>3</sup>J. Dutton, *Phys. Chem. Ref. Data* **4**, 577 (1975).

<sup>4</sup>H. N. Kucukarpaci and J. Lucas, *J. Phys. D* **12**, 2123 (1979).

<sup>5</sup>J. W. Gallagher, E. C. Beaty, J. Dutton, and L. C. Pitchford,

*J. Chem. Ref. Data* **12**, 109 (1983).

<sup>6</sup>A. Von Engel, *Ionized Gases* (Oxford University, London, 1965).

<sup>7</sup>M. Ohuchi and T. Kutoba, *J. Phys. D* **16**, 1705 (1983).

<sup>8</sup>J. P. Boeuf and E. Marode, *J. Phys. D* **15**, 2169 (1982).

<sup>9</sup>A. L. Ward, *Phys. Rev.* **112**, 1852 (1958).